arXiv:1606.09203v2 [physics.chem-ph] 6 Jul 2016

First principles simulations of a bias-dependent electrochemical cell

Luana S. Pedroza,[1,2,*] Pedro Brandimarte,[3,4] Alexandre Reily Rocha,[5] and M.-V. Fernández-Serra[6,7]

[1] *ICTP South American Institute for Fundamental Research, Instituto de Física Teórica, Universidade Estadual Paulista, São Paulo SP 01140-070, Brazil*
[2] *Centro de Ciências Naturais e Humanas, Universidade Federal do ABC, Santo André, São Paulo, Brazil 09210-170*
[3] *Centro de Física de Materiales, 20018 Donostia-San Sebastián, Basque Country, Spain*
[4] *Donostia International Physics Center, 20018 Donostia-San Sebastián, Basque Country, Spain*
[5] *Instituto de Física Teórica, Universidade Estadual Paulista, São Paulo, São Paulo SP 01140-070, Brazil*
[6] *Department of Physics and Astronomy, Stony Brook University, Stony Brook, New York 11794-3800, USA*
[7] *Institute for Advanced Computational Sciences, Stony Brook University, Stony Brook, New York 11794-3800, USA*

(Dated: July 7, 2016)

Understanding the local structure of liquid water at the interfaces of metallic electrodes is a key problem in aqueous-based electrochemistry. Notably the system is under an external potential bias, which makes the task of simulating this setup difficult. To correctly compute the effect of an external bias potential applied to electrodes, we combine density functional theory and non-equilibrium Green's functions methods. Our method now allows to explicitly consider an external applied bias, in direct correspondence to the experiments. In this work, we apply this methodology to study the electronic properties and atomic forces of one water molecule at the interface of gold electrodes. We find that, as expected, the water molecule is sensitive to the sign and magnitude of the applied bias.

Following the need for new - and renewable - sources of energy worldwide, fuel cells using electrocatalysts can be thought of as a viable option [1, 2]. The interface between a metal (electrode) and water in these systems is the electrochemical central point, since it is the region where charge transfer can take place. Understanding it is also an essential requisite for predicting the correspondence between the macroscopic voltage and the microscopic interfacial charge distribution in electrochemical fuel cells [3, 4]. This reactivity is governed by the explicit atomic and electronic structure built at the interface as a response to external conditions, such as an applied potential.

The advance in experimental techniques for studying surfaces in the last decades started to provide important results concerning the local structure of water at interfaces, revealing a bias-dependent behavior [5–7]. Notably, in a more realistic system applied to catalysis, the metal will be at a given potential. From a theoretical perspective it makes the task of simulating this setup difficult [8]. In fact, an accurate calculation of the electrostatic potential at electrically biased metal-electrolyte interfaces is a challenge for periodic *ab initio* simulations [9, 10].

One possibility to describe this electrochemical cell is to account for the polarization of the metal by charging each atom on the electrode, enforcing a constant potential and using the image charges method [11–13]. Although they can provide interesting insights into the problem, the description is limited to the use of empirical models. Neurock's studies of the water/metal interface in the presence of an applied potential [14, 15] are among the first ones that have used Density Functional Theory (DFT) [16, 17] to address this problem. The resulting electrode potential – which is related to the Fermi energy of the system – is compared to an internal reference potential by artificially inserting a vacuum layer into the center of the solution region. To be able to fully compute all these energies when the system is charged, the water molecules in the center of the liquid layer are usually held fixed during the optimization of the charged systems. More recently, N. Bonnet *et al.* proposed a methodology where an external potentiostat is added to the system [18]. The idea is to use the potential energy of a fictitious system, in a similar way to what is done in Car-Parrinello first-principles molecular dynamics.

A. Huzayyin [19] and coworkers studied the interaction of a water molecule with an Au(111)-terminated slab in the presence of an external electric field. Their results show that the structure of the H_2O molecule at the metal interface is dependent on the sign and magnitude of the applied field. However, their calculations require the inclusion of a second water molecule at the periodic metal surface to ensure the symmetry of the full system, which may influence the results for polarized structures. Therefore, current methodologies attempt to simulate the effect of finite bias at the metal by controlling their charge (adding/subtracting electrons), whereas in experiments the potential is the quantity that is controlled.

The electrochemical cell can be thought of as two metallic electrodes which act as charge reservoirs, with the two metal plates separated by a solution (mostly composed by water). This is an arrangement analogous to the one encountered in simulations of electronic transport: a central scattering region coupled to electrodes [20–22]. Thus, we propose in this work, as an alternative, to use open boundary conditions by employing the non-equilibrium Green's function (NEGF) method combined with DFT to properly compute the effect of an external bias potential applied to electrodes. While stan-

dard DFT implementations are not suited to treat extended systems under an external bias, NEGF has been designed to treat out-of-equilibrium situations. Their combination has been developed over the past decade to describe current-voltage characteristics of nanoscopic systems [21–23]. It treats an open system under the influence of an external bias, and albeit dynamics - or forces - is typically ignored in such systems, it can be incorporated into the methodology. In this work, we apply this framework to a system consisting of a single water molecule on top of a Au(111) surface, at different configurations and as a function of an external voltage.

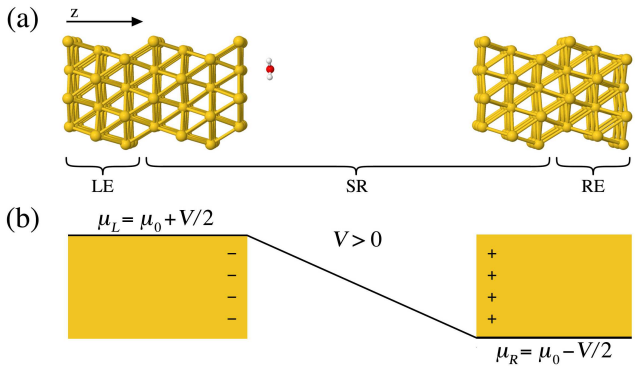

FIG. 1. (Color online) (a) Schematic view of the metal-water system used for the non-equilibrium calculations; the left (right) electrodes (LE/RE) and scattering region (SR) are indicated. (b) Sketch of the effect of a positive bias potential on a parallel plate capacitor; the corresponding charge accumulated in each plate as well as the bias ramp are shown.

In what has become an usual approach in electronic transport calculations, the system is divided into three regions: electrodes (left and right, L/R) and scattering region (SR) [24]. In the case of our metal-water system we have to frame it into an analogous arrangement. Therefore, the interfacial region (metal-water-metal) represents the scattering region. The first few layers of the metal at the interface need to be considered part of the scattering region as we require that the charge density at the edge of the scattering region resembles the one of the bulk metal. Then, the electronic charge distributions in the electrodes, left and right, correspond to the bulk phases of the same material to a prescribed numerical accuracy. A representation of the typical arrangement used in our calculations is shown in Figure 1 (a).

When a finite bias is applied to the electrodes the problem becomes a non-equilibrium one. The electrodes are then described by different chemical potentials and current, in principle, can flow. Within the non-equilibrium Green's function approach, if the Hamiltonian can be cast in a bilinear form, the entire problem can be treated in terms of a single Green's function; in our case the retarded Green's function for the scattering region,

$$G^{(\mathrm{E,V})} = lim_{\eta\to 0}\left[\epsilon^{+} S_{\mathrm{SR}} - H_{\mathrm{SR}}[n] - \Sigma_{\mathrm{L}}(E,V) - \Sigma_{\mathrm{R}}(E,V)\right] , \quad (1)$$

where $\epsilon^{+} = E + i\eta$, S_{SR} is the overlap matrix and $H_{\mathrm{SR}}[n]$ is a Hamiltonian which is a functional of the charge density, $n(\vec{r})$. Here the Hamiltonian is taken as the Kohn-Sham (KS) hamiltonian from DFT. The effects of the electrodes are introduced in the form of the self-energies $\Sigma_{\mathrm{L/R}}$, which are obtained by integrating out the degrees of freedom of the leads. As the electrodes are considered to be good metals, the effect of the bias on the left and the right electrodes corresponds to a rigid shift ($\pm V/2$) of the self-energies, setting the boundary condition (illustrated in Fig. 1 (b) for a positive bias).

Once the Green's function of the SR is calculated, all the observables of the system can be computed. In particular the density matrix is expressed as:

$$D_{\mu\nu} = \int_{-\infty}^{\infty} d\epsilon [\rho^{L}_{\mu\nu} f(\epsilon - \mu_L) + \rho^{R}_{\mu\nu} f(\epsilon - \mu_R)] \quad (2)$$

where $f(\epsilon) = 1/(1+e^{+\epsilon/kT})$ is the Fermi distribution and μ_R and μ_L are the electrochemical potentials of the right and left electrodes ($\mu_{L/R} = \mu_0 \pm V/2$), that defines the bias: $V = \mu_L - \mu_R$. Finally

$$\rho^{L/R} = G(E)\,\Gamma_{L/R}(E)\,G^{\dagger}(E) \quad (3)$$

is the electrode spectral density matrix, obtained from the Green's function of the SR and the left (right) coupling matrices, $\Gamma_{L/R} = i\left[\Sigma_{L/R}(E) - \Sigma^{\dagger}_{L/R}(E)\right]$. From the density matrix, the KS hamiltonian can be computed. The procedure is then repeated until self consistency is achieved.

Within the ground state DFT framework, the computation of forces on the nuclei is theoretically well founded thanks to the Hellman-Feynman theorem, and the forces are obtained via the derivative of the total energy. Using a set of localized basis functions the force is decomposed in two terms: one that originates from the derivative of the energy of the occupied eigenstates (band structure contribution) and a second one that contains the remaining contributions to the energy. The former one is given by:

$$\vec{F}_{BS} = -\sum_{\mu\nu} D_{\mu\nu}\frac{\partial H_{\mu\nu}}{\partial \vec{R}_I} + \Omega_{\mu\nu}\frac{\partial S_{\mu\nu}}{\partial \vec{R}_I} . \quad (4)$$

where $D_{\mu\nu}$ is the density matrix and $\Omega_{\mu\nu}$ is the energy density matrix ($\Omega_{\mu\nu} = \sum_i \epsilon_i f(\epsilon_i)\Psi_{i\mu}\Psi^{*}_{i\nu}$). The situation is more complex out of equilibrium, where the Hellman-Feynman theorem does not apply[25]. Recently, it was shown that the forces can actually be obtained by the time derivative of the expectation value of the ionic momentum operators[25, 26]:

$$\vec{F}_I = \frac{\partial}{\partial t}\langle\Psi(t)| - i\hbar\frac{\partial}{\partial \vec{R}_I}|\Psi(t)\rangle . \quad (5)$$

For steady-state transport problems, however, the final form for the force is equivalent to the equilibrium case,

$$\vec{F}_I = -\frac{\partial \langle \Psi | H | \Psi \rangle}{\partial \vec{R}_I} \ , \tag{6}$$

which can be expressed by Eq. 4, replacing now the ground state density matrix and energy density matrix by the out-of-equilibrium ones, now obtained in terms of the retarded Green's function.

One important point that still remains is how well defined are the forces when current flows in the system [27]. In our case, however, the gap in the scattering region – the band gap of water – is large enough (~ 8 eV) to ensure that no current will flow through the arrangement. In that sense, current-induced forces will not be present in our problem. This remains true for the simulation of ionic electrolytes, where ionic currents will exist, but no electronic currents.

The above methodology was implemented in the Smeagol code [22, 23] which is bundled with Siesta [28, 29]. In the same way that relaxation and *ab initio* molecular dynamics can be performed within DFT, one can use the code to do the same for out-of-equilibrium systems.

In this work, we have used two different gradient-dependent exchange-correlation (XC) functionals: PBE [30] and vdW-DF^{PBE}, which includes van der Waals corrections. The vdW-DF^{PBE} is a modified version of the original vdW-DF functional [31], in which the revPBE local term was replaced by PBE [32]. The core electrons were described by norm-conserving pseudopotentials in the Troullier-Martins form [33]. A basis set of numerical atomic orbitals with double-ζ polarization (DZP) was used to describe the valence electrons. For both metal and water the basis set was variationally optimized and ensured that our results (Au lattice parameter, water-metal geometry) are in agreement with plane-wave calculations. All the atoms were allowed to move during the geometrical optimization, using the conjugate gradient algorithm and with a 0.005 eV/Å tolerance criteria on the forces.

For the non-equilibrium calculations, each metal slab has 3 layers of 12 Au atoms, with size 10.29×9.89 Å in the plane perpendicular to the transport direction. The water molecule is placed close to one metal surface (the one defined as left). In order to minimize the interaction between the surfaces, the right and left side are 20 Å apart. The electrodes, connected to the scattering region, consist of 3 Au layers each (left and right). Figure 1 shows a schematic view of the system and its components.

Before applying a bias at the electrodes it is important to characterise the ground state configuration of the metal-water system. This was done using a Au 2x2x4 supercell. Our results show that the most stable configuration of one water molecule on top of the Au(111) surface is the "flat" one (i.e. the molecule dipole moment is almost parallel to the surface plane), in agreement to previous reported calculations [34, 35]. The molecular plane is slightly tilted with respect to the metal plane, with $\alpha = 3^o$ (α being the angle between the molecular plane and the surface normal) and the distance between Au and O is 2.79 Å. This structure is illustrated in the inset of Fig. 2 (b). We have also relaxed the metal-water-metal structure using the NEGF formalism at zero bias, with similar results to the ones obtained with standard DFT. As expected for Au/H_2O interaction, vdW corrections do not alter significantly the geometrical results [36, 37].

It is worth mentioning that the potential energy surface (PES) for this system is very smooth in the region of the water on top of Au. For instance, the energy difference between the configuration where the molecule is flat compared to the one where it has the hydrogens pointing down (towards the metal) is only ~ 0.06 eV. Therefore, we also considered an extra four different configurations for the water molecule, corresponding to rigid rotations of the ground state structure. The geometries are labeled according to their orientation: "up" (hydrogens pointing away from the metal), "down" (hydrogens pointing towards the metal), "perpendicular" ($\alpha = 90^o$ and $\theta = 90^o$); and "flat-up" (one hydrogen higher than the flat configuration, with $\alpha = 8^o$ and $\theta = 157^o$). The angle θ corresponds to the angle between a vector perpendicular to the molecular plane and the normal to the surface.

In order to analyze the effect of different bias voltages (magnitude and sign) on the molecule as a function of the water position, we performed non-equilibrium calculations for all water structures (geometries shown in the insets of Fig. 2). For each configuration, we started at the ground state Au-O distance ($z = 2.79$ Å, which corresponds to zero in the plots) and increased/decreased this distance by -0.5 to +2.0 Å , and performed a single point calculation. At each point the forces on the atoms were evaluated for each applied bias. Since the water molecule is placed close to one metal surface, we observe that the potential in the water molecule follows closely that of the surface. Therefore, the bias we are indicating in the plots corresponds to $V/2$, as it indicates the potential effectively acting on the molecule. The results for the force on the center of mass of the molecule are shown in Fig. 2 for all orientations.

In general, we observed that low bias (-0.5 and +0.5 V) has a small effect on the forces, independently of the water configuration. However, as we increase the applied bias we observe that the forces close to the minimum are modified. In particular, this effect is more evident for the flat molecule (Fig. 2 (a), (b)) and for configurations where the oxygen is facing the metal, due to strong interaction between the oxygen-b_1 orbital of the water molecule and the metal orbitals [38, 39].

In Fig. 2 it is possible to observe that there is a ten-

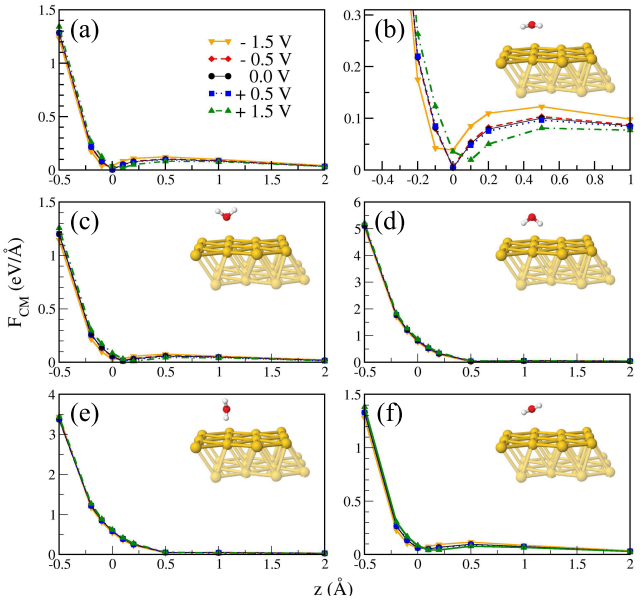

FIG. 2. (Color online) Force at the center of mass as a function of the vertical displacement for different water configurations: (a) "flat", (b) minimum region for the "flat" molecule, (c) "up", (d) "down", (e) "perpendicular" and (f) "flat-up". The vertical displacement is given with respect to the Au-O distance at ground state.

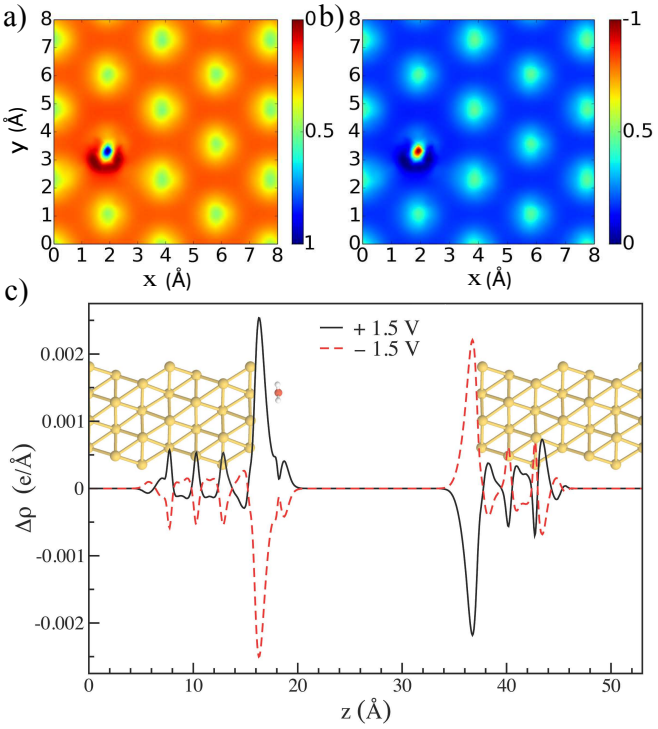

FIG. 3. (Color online) *Flat configuration.* Relative change in charge density in comparison to the zero bias for +1.5 V (a) and -1.5 V (b), taken at the plane of the water molecule. (c)Laterally averaged difference in charge density in comparison to the zero bias: in black for +1.5 V and in red for -1.5 V; the water-metal system indicates the position of the atoms.

dency to modify the position of the minimum configuration when the bias is applied. Moreover, this modification is dependent on the sign of the bias and it is asymmetric with respect to positive and negative values. This behavior is similar to what is verified when an electric field is applied [19, 40]: The molecule tends to get closer to the metal when the bias is negative and moves away from the metal with positive bias. A similar trend can be observed for configurations "up" and "flat-up" shown in Figures 2 (c) and (f), respectively. For "down" and "perpendicular" configurations the molecule is essentially unbound at this distance (Fig. 2 (d) and (e), respectively).

The water-Au interaction is mostly electrostatic in nature, and there is almost no charge transfer between water and the metal in the neutral case [41]. At the same time, the effect of the bias on configurations can be understood in terms of a combination of Pauli repulsion and charging of the surface. Figure 3 shows the difference in charge density for different bias compared to the zero-bias case on the plane of the water molecule. Figures 3(a-b) indicate that most of the change in charge on the molecule is located on the oxygen. That transfer is small, however, as seen in Fig. 3(c), and the direction of the water molecule's dipole is not altered when the bias is included (both cases). Thus, the picture that arises is the following: for positive bias the left hand side surface becomes negatively charged and tends to repel the negatively charged oxygen. At the same time as a small amount of charge is transferred to the oxygen the overlap between oxygen orbitals and gold surface orbitals tend to move the molecule away due to Pauli repulsion. The opposite behavior is expected for negative bias.

Finally, a similar behavior was also observed when vdW corrections are included for the flat configuration, as shown in SI [42]. In agreement to previous work [41], we note that the vdW functional does not change significantly the water-Au interaction. We observe, however, that the barrier in all cases increases slightly for higher distances; this is true for zero as well as finite (positive or negative) bias. This means that, although the equilibrium position of the molecule does not depend on the choice of XC functional, the restoration force is larger when we include vdW interaction.

The inclusion of electronic effects via DFT in the description of water-metal interactions is important to advance in the comprehension of the local structure of water at an electrochemical interface. In this work we showed how DFT and NEGF can be used to describe water-metal systems under an external bias potential. This methodology now allows to properly calculate the forces and therefore perform dynamics of water-metal systems out of equilibrium. Here, we presented how the magnitude

and sign of the bias alters the interaction of a prototype system of one water molecule on top of an Au(111) surface. The external bias changes both the external position and alignment of the molecule with the surface, thus indicating that the introduction of an external bias has a significant influence on the microscopic structure of molecules at a metallic interface.

ACKNOWLEDGMENTS

This research used computational resources at the Center for Functional Nanomaterials, Brookhaven National Laboratory, which is supported by the US Department of Energy under Contract No. DE-AC02-98CH10886. The work was funded by DOE Early Career Award No. de-sc0003871. L.S.P. and A.R.R. also acknowledge financial support from ICTP-SAIFR (FAPESP project No. 2011/11973-4) and the ICTP-Simons Associate Scheme. P.B. acknowledge financial support from FP7 FET-ICT "Planar Atomic and Molecular Scale devices" (PAMS) project (funded by the European Commission under contract No. 610446), the Spanish Ministerio de Economia y Competitividad (MINECO) (Grant No. MAT2013-46593-C6-2-P) and the Basque Dep. de Educacin and the UPV/EHU (Grant No. IT-756-13).

* To whom correspondence should be addressed: l.pedroza@ufabc.edu.br

[1] J. K. Norskov, T. Bligaard, J. Rossmeisl, and C. H. Christensen, Nature Chemistry **1**, 37 (2009).
[2] J. Greeley and N. M. Markovic, Energy Environ. Sci. **5**, 9246 (2012).
[3] A. Hodgson and S. Haq, Surf. Sci. Rep. **64**, 381 (2009).
[4] P. A. Thiel and T. E. Madley, Surf. Sci. Rep. **7**, 211 (1987).
[5] M. F. Toney, J. N. Howard, J. Richer, G. L. Borges, J. G. Gordon, O. R. Meiroy, D. G. Wiesler, D. Yee, and L. B. Sorensen, Nature **368**, 444 (1994).
[6] J.-J. Velasco-Velez, C. H. Wu, T. A. Pascal, L. F. Wan, J. Guo, D. Prendergast, and M. Salmeron, Science **346**, 831 (2014).
[7] K. Ataka, T. Yotsuyanagi, and M. Osawa, J. Phys. Chem. **100**, 10664 (1996).
[8] M. Nielsen, M. E. Björketun, M. H. Hansen, and J. Rossmeisl, Surface Science **631**, 2 (2015).
[9] F. Calle-Vallejo and M. T. M. Koper, Electrochimica Acta **84**, 3 (2012).
[10] J. Cheng and M. Sprik, Phys. Chem. Chem. Phys. **14**, 11245 (2012).
[11] J. I. Siepmann and M. Sprik, J. Chem. Phys. **102**, 511 (1995).
[12] A. P. Willard, S. K. Reed, P. A. Madden, and D. Chandler, Faraday Discuss. **141**, 423 (2009).
[13] M. K. Petersen, R. Kumar, H. S. White, and G. A. Voth, J. Phys. Chem. C **116**, 4903 (2012).
[14] C. D. Taylor, S. A. Wasileski, J.-S. Filhol, and M. Neurock, Phys. Rev. B **73**, 165402 (2006).
[15] J.-S. Filhol and M. Neurock, Ang. Chem. Int. Ed. **45**, 402 (2006).
[16] P. Hohenberg and W. Kohn, Phys. Rev. B **136**, 864 (1964).
[17] W. Kohn and L. J. Sham, Phys. Rev. A **140**, 1133 (1965).
[18] N. Bonnet, T. Morishita, O. Sugino, and M. Otani, Phys. Rev. Lett. **109**, 266101 (2012).
[19] A. Huzayyin, J. H. Chang, K. Lian, and F. Dawson, J. Phys. Chem. C **118**, 3459 (2014).
[20] S. Datta, *Quantum Phenomena. Modular Series on Solid State Devices - Vol. VIII* (Addison-Wesley, 1989).
[21] M. Brandbyge, J.-L. Mozos, P. Ordejón, J. Taylor, and K. Stokbro, Phys. Rev. B **65**, 165401 (2002).
[22] A. R. Rocha, V. M. García-Suárez, S. W. Bailey, C. J. Lambert, J. Ferrer, and S. Sanvito, Phys. Rev. B **73**, 085414 (2006).
[23] A. R. Rocha, V. M. García-Suárez, S. W. Bailey, C. J. Lambert, J. Ferrer, and S. Sanvito, Nature Materials **4**, 335 (2005).
[24] C. Caroli, R. Combescot, P. Nozieres, and D. Saint-James, J. Phys. C **4**, 916 (1971).
[25] M. Di Ventra and S. T. Pantelides, Phys. Rev. B **61**, 16207 (2000).
[26] R. Zhang, I. Rungger, S. Sanvito, and S. Hou, Phys. Rev. B **84**, 085445 (2011).
[27] T. N. Todorov, D. Dundas, and E. J. McEniry, Phys. Rev. B **81**, 075416 (2010).
[28] P. Ordejón, E. Artacho, and J. M. Soler, Phys. Rev. B **53**, 10441 (1996).
[29] J. M. Soler, E. Artacho, J. D. Gale, A. García, J. Junquera, P.Ordejón, and D. Sánchez-Portal, J. Phys. Condens. Matter. **14**, 2745 (2002).
[30] J. P. Perdew, K. Burke, and M. Ernzerhof, Phys. Rev. Lett. **77**, 3865 (1996).
[31] M. Dion, H. Rydberg, E. Schroder, D. C. Langreth, and B. I. Lundqvist, Phys. Rev. Lett. **92**, 246401 (2004).
[32] J. Wand, G. Roman-Perez, J. Soler, E. Artacho, and M. V. Fernandez-Serra, J. Chem. Phys. **134**, 024516 (2011).
[33] N. Troullier and J. L. Martins, Phys. Rev. B **43**, 1993 (1991).
[34] A. Michaelides, V. A. Ranea, P. L. de Andres, and D. A. King, Phys. Rev. Lett. **90**, 216102 (2003).
[35] G. Cicero, A. Calzolari, S. Corni, and A. Catellani, J. Phys. Chem. Lett. **2**, 2582 (2011).
[36] J. Carrasco, J. Klimes, and A. Michaelides, J. Chem. Phys. **138**, 024708 (2013).
[37] R. Nadler and J. F. Sanz, J. Chem. Phys. **137**, 114709 (2012).
[38] A. Poissier, S. Ganeshan, and M. V. Fernandez-Serra, Phys. Chem. Chem. Phys. **13**, 3375 (2011).
[39] J. Carrasco, A. Michaelides, and M. Scheffler, J. Chem. Phys. **130**, 184707 (2009).
[40] Note that the positive bias is defined when we have net negative charge on the surface. Therefore, this situation corresponds to the negative electric field in Ref.[19].
[41] L. S. Pedroza, A. Poissier, and M.-V. Fernández-Serra, J. Chem. Phys. **142**, 034706 (2015).
[42] See supplemental material at [url] for bias-dependent forces including vdW corrections.